First-Principles Simulations of Boron Diffusion in Graphite

I. Suarez-Martinez,* A. A. El-Barbary, G. Savini, and M. I. Heggie

Department of Chemistry, School of Life Science, University of Sussex, Falmer, Brighton BN1 9QJ, United Kingdom

(Received 26 July 2006; published 4 January 2007)

Boron strongly modifies electronic and diffusion properties of graphite. We report the first *ab initio* study of boron interaction with the point defects in graphite, which includes structures, thermodynamics, and diffusion. A number of possible diffusion mechanisms of boron in graphite are suggested. We conclude that boron diffuses in graphite by a kick-out mechanism. This mechanism explains the common activation energy, but large magnitude difference, for the rate of boron diffusion parallel and perpendicular to the basal plane.

DOI: 10.1103/PhysRevLett.98.015501 PACS numbers: 61.72.Ji, 28.41.Pa, 61.80.Az, 66.30.Jt

The structure of graphite is known to accept many impurities at interlayer positions, but boron is the only substitutional impurity routinely found in graphite. The maximum thermal solubility of boron in the graphite lattice is 2.35 at. % at 2350 °C [1]. Substitutional boron in graphite is detected by gold nucleation or better, by etching followed by etch pit decoration [2].

Graphite has tremendous technological importance from electrode material to nuclear moderator, and when impregnated with boron it can be used as a radiation shield and control rod material. This has given rise to a substantial amount of literature dealing with radiation damage, often with boron as a deliberate contaminant in order to accelerate the damage rate through the ^{11}B isotope which has a large cross section for neutron capture [3]. Nowadays, the most important commercial application of B-doped graphite is as anode material in advanced Li-ion batteries, widely used in mobiles and laptop computers [4,5].

In order to reconcile the very low interstitial migration energy (historically thought to be in the range 0.02–0.4 eV [6]) with rate measurements on prismatic loop growth in radiation damage experiments, boron has been invoked as a trap for the self-interstitial. Measurements of the nucleation and growth of interstitial loops in highly oriented pyrolytic graphite (HOPG) during irradiation at different temperatures revealed Arrhenius dependences of 1.2 eV [7] and 1.17 eV [8].

From the prefactor, an entropy of migration for the diffusing species of $6k_B$ is deduced [8]. Reference [8] argues that this is the migration energy of a small cluster of C (e.g., C_2), while the Ref. [7] rules out this explanation on chemical kinetic grounds and argues that it is trap-limited interstitial diffusion. The trap was thought to be boron, and the functional dependence of nucleation density with boron concentration was correctly predicted [7]. The trap-limited migration energy was given as $E_B + E_{m,i}$, where E_B is the boron trapping energy and $E_{m,i}$, the migration energy of the self-interstitial. An estimate for E_B via another feature in the loop growth behavior gave 1.45 eV [7].

Observations of *in situ* annealing of electron radiation damage confirm a high interstitial migration energy (0.8–0.9 eV), as obtained in fitting a model to dimensional change (0.86 eV) [9]. Post-irradiation annealing on low T irradiation yields defect processes with activation energies 0.5, 0.9, and 1.2 eV [10,11].

One of the fundamental unresolved topics is that the activation energy for boron diffusion in graphite is very close to that of self-diffusion, as Table I shows. The similarity of activation energy seems to imply a common mechanism.

We have undertaken a density functional study of boron within graphite, using the AIMPRO supercell code within the local density functional formalism fitting the charge density to plane waves with an energy cutoff of 200 Ry. Atom-centered Gaussian basis functions are used to construct the many-electron wave function. These functions are labeled by four orbital symbols, where for each symbol all angular momenta are allowed up to maxima p ($l = 0, 1$) and d ($l = 0, 1, 2$), respectively. Following this nomenclature, the basis sets $pdpp$ and $ddpp$ are used for C and B, respectively. A Bloch sum of these functions is performed over the lattice vectors to satisfy the periodic boundary conditions of the supercell. These basis sets have been tested by comparison of the calculated band structure and lattice parameters with the experimental values. Charge density oscillations in part-filled degenerate orbitals during the self-consistency cycle were damped using a Fermi occupation function with $kT = 0.04$ eV. For further details of the general method, see Ref. [13].

TABLE I. Experimental values for boron [2] and self-diffusion [12] constants and activation energies in graphite.

Diffusion	D_o (cm^2/s)	E_a (eV)
Boron along **a**	6320	6.78
Boron along **c**	7.1	6.61
Self-diffusion	6.3	6.99

Calculations are performed on a $4 \times 4 \times 1$ unit cell of hexagonal graphite, with Brillouin zone sampling using $2 \times 2 \times 2$ k points within the Monkhorst-Pack scheme [14]. Unless otherwise stated, the calculations have been performed in the same size of supercell with the same density of k points. In the analysis that follows, a perfect crystal of AB graphite of 64 C atoms (2 layers) and boron-rhombohedral solid were taken as the standard states of carbon and boron.

The AIMPRO code has been employed to examine the process of diffusion by a search for saddle points. When the saddle point structure presents higher symmetry than the ground states, symmetry constraints are used. A starting structure of the correct symmetry can be relaxed subject to retaining that symmetry. Verification of the path is demonstrated by breaking the symmetry. This method has been used in the location of the saddle point of the migration of boron as an interstitial. Orthogonality constraints are used as well. In this method, a vector is defined for the atoms involved in the diffusion. The vector is obtained as the difference between the relaxed initial and final states. The system is stepped along the vector and allowed to relax at each step.

In this Letter we model the structure, energy, and migration of the boron substitutional (B_s), the boron interstitial (B_i), and the interaction of B_s with the vacancy (B_s:V) and self-interstitial (B_s:I), to determine the boron diffusion mechanism in graphite and its effect on prismatic loop development.

The substitution of boron in the hexagonal net of graphite is well known to occur at low doping levels [1]. The substitution is accompanied by an expansion in the basal lattice due to longer B-C bonds [1].

Substitutional boron is threefold coordinated. The possibility of a nonplanar C_{3v} configuration has been suggested [15], but the current calculations find the planar D_{3h} configuration lower in energy, even from a C_{3v} starting state. The B-C bond distances of 1.47 Å are accommodated in the graphite lattice by deforming the hexagons around the B substitution without losing the planar configuration and increasing the basal lattice parameter by 0.25% in our cells. However, the substitution of boron atoms in curved carbon structures seems to be easier. The substitution of boron in fullerene C_{60} is 0.07 eV lower in energy than in graphite, where the B-C bonds are 1.50 and 1.53 Å.

The monovacancy atomic structure has been determined from first principles elsewhere [16]. The ground-state structure is a time-average combination of three symmetry breaking Jahn-Teller distortion configurations. The symmetry is reduced from D_{3h} to C_s by splitting the asymmetrically occupied $2E'\sigma$ states in order to lower the total energy. The Jahn-Teller distortion forces a weak reconstructed bond between two of the dangling carbons and displaces the third dangling carbon out of the atomic layers by 0.47 Å in local-density approximation [16] (somewhat less in spin polarized calculations [17]). The distortion does not occur in the boron:vacancy (B_s:V) complex. Boron atoms have one electron fewer than carbon, leaving the $2E'\sigma$ states unoccupied. The (B_s:V) complex does not suffer Jahn-Teller distortion and remains C_{2v} planar and unreconstructed, as Fig. 1 shows.

Similarly to the (B_s:V) complex, the boron:carbon interstitial (B_s:I) complex was studied. The ground-state atomic structure for a carbon interstitial has been determined from first principles elsewhere [18]. Graphite self-interstitial defects tend to form cross-links between the atomic layers. The most stable structure is a fourfold coordinated "spiro" configuration, which is made possible by basal shear of half a bond length in magnitude (0.71 Å) in the $\langle 1\bar{1}00 \rangle$ direction [18]. The (B_s:I) complex and boron interstitial structures are simulated by substituting one of the host carbon atoms bonded to the interstitial atom or the interstitial atom itself, respectively, by boron. The optimized structures are very similar to the spiro self-interstitial with the difference of longer B-C bond lengths, as Fig. 2 shows.

Table II gives the formation energies of all structures we have studied. Where comparisons with experiment is possible, they are sensible. Electron energy loss spectroscopy (EELS) reveals that boron is threefold coordinated at all but the highest concentration [19] (whereupon it presumably can take on the B_i structure). The dissociation energy for the (B_s:V) complex into its isolated components B_s and V is 2.7 eV. In the same way, the dissociation energy for the (B_s:I) complex is 1.1 eV. Boron produces an attractive potential well in the potential energy surface for the vacancy and for the interstitial, making more likely the migration of the defect in the direction of the boron substitution, even if the boron is at the position of second or third neighbor.

The boron interstitial is fourfold coordinated. There are two possible configurations: canted, in the AB stacking, and spiro in AB graphite which has a 0.7 Å layer shift. The spiro configuration is the lowest in energy for the unit cell used (64 atom in 2 layers); however, for bigger unit cells the lowest energy state may be the canted configuration as the stacking fault energy is increased. Taking a stacking fault energy for AB graphite shifted by 0.7 Å to be

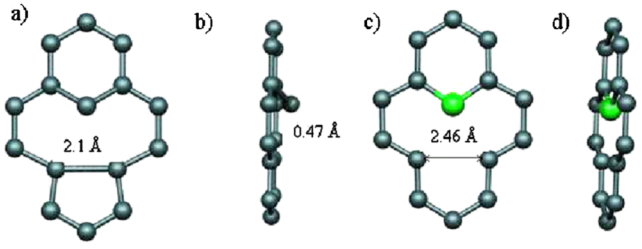

FIG. 1 (color online). (a) Top and (b) side views of the ground state for the monovacancy structure, C_s. (c) Top and (d) side views of the ground state for (B_s:V) complex structure, C_{2v}.

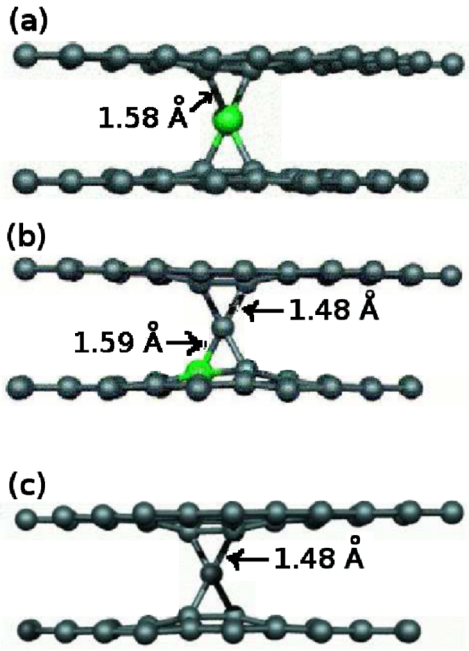

FIG. 2 (color online). (a) Boron interstitial (B_i) structure, (b) boron:interstitial (B_s:I) complex structure, and (c) self-interstitial (I) structure. The structures are AB graphite shifted by 0.71 Å in the $\langle 1\bar{1}00\rangle$ direction.

1.06 meV/Å^2 [18], for boron concentrations lower than 3.4% (where the area between boron atoms is bigger than 83 Å^2), boron interstitial atoms are expected to be in a canted configuration.

Experimental values for the activation energy and diffusion constant of boron in graphite were measured by Hennig [2] (see Table I), although no mechanism was suggested. He investigated the mobility of substitutional boron in single crystals of graphite by etch-decoration technique. The diffusion was determined by the ''constant-source'' method. A number of possible diffusion mechanisms can be postulated [20]. Here we investigated possible mechanisms for boron diffusion in graphite crystals, in plane (direct-exchange and vacancy mechanism), out of plane (interstitialcy, or kick-out, and direct-exchange mechanism), and in the interlayer space (boron interstitial mechanism).

The direct-exchange mechanism involves the rotation of a pair of bonded atoms (in plane) or atoms from different layers (out of plane). In-plane direct-exchange mechanism has been suggested as a self-diffusion mechanism in graphite, although it was ruled out because of its high energy barrier [21,22]. The calculated barrier for the in-plane direct-exchange diffusion of boron is 7.5 eV. Out-of-plane direct-exchange implies the rotation of two atoms from different layers and lying one above the other (α sites). The pair undergoes rotation through three different angles, finding the highest saddle point at 12.3 eV, for the case of carbon, and 10.8 eV for the case of boron.

The diffusion of boron via vacancies involves first the formation of the complex (B_s:V) and a number of intermediate metastable structures. The metastable structure with the highest energy in this path is the boron:vacancy complex in the *cis* configuration (third neighbor with the shortest distance), with an energy of 8.96 eV. This mechanism is therefore ruled out as the boron diffusion mechanism.

Boron and carbon present a very similar size; therefore an interstitialcy mechanism seems very likely to be the diffusion mechanism normal to the basal plane. The interstitial atom pushes one of the atoms which is bonded to it into the next interlayer space. A schematic representation of this mechanism is shown in Fig. 3. From a B_s:I complex, the carbon interstitial atom pushes the boron atom out of the basal plane. For diffusion perpendicular to the basal plane, the boron atom must kick back into the layer. However, for diffusion parallel to the layer, the boron atom must diffuse in the interlayer space as an interstitial (interstitial mechanism) and then kick back in.

The mechanism goes through a metastable configuration, here called B_s:I split (see Fig. 3). This configuration is slightly more stable for an α position than a β position as it has an extra bond with the layer above. Once the boron atom is placed in the interlayer space, it will diffuse parallel to the basal plane. When boron is placed in the interstitial site, it can diffuse as an interstitial with an energy barrier of 0.8 eV, i.e.,

TABLE II. Boron and carbon defect energies (eV): formation energy (E_f), migration energy (E_m), and dissociation energy (E_d) in 64 atoms supercell.

Structure	E_f	E_m	E_d
Monovacancy	8.4	1.7	NA
B_s:V complex	7.1	1.7	2.7
B_s:I complex	5.7	1.3	1.1
Carbon interstitial	5.4	0.9	NA
Boron interstitial	4.5	0.8	NA
Boron substitutional	1.4	See Table III.	NA

[a]The migration energy for a complex is given as the activation barrier to the first dissociation step.
[b]The dissociation energy is the difference in energy between the complex and its constituent parts at infinite separation in graphite.

TABLE III. Summary of theoretical activation energies (E_a) for possible mechanisms of boron substitutional diffusion in graphite.

Diffusion mechanism	E_a (eV)
In-plane direct exchange	7.5
Out-of-plane direct exchange	10.8
Via vacancy	9.0
Kick-out	6.8

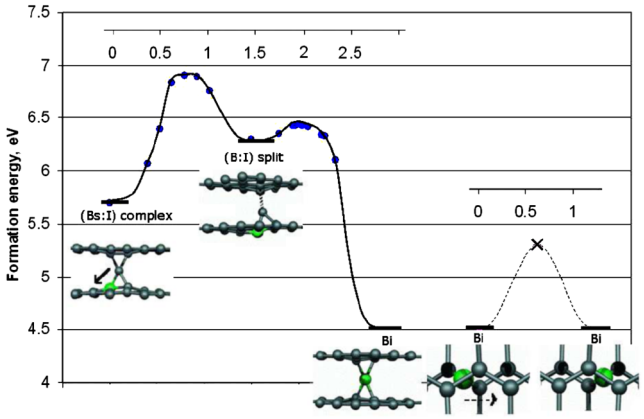

FIG. 3 (color online). Proposed model of boron diffusion in graphite. The solid line picks out the kick-out mechanism and the dashed line the diffusion of the boron as an interstitial. The x axis for each mechanism is the displacement, in Å of the diffusing atoms along the diffusion direction.

$E_a^{\text{via interstitial}}$-$E_{\text{formation}}^{B_i}$. The activation barrier for this mechanism is determined by the highest transition state of the entire path, which for this mechanism is the saddle point at 6.8 eV. This barrier is the lowest which explains both parallel and perpendicular diffusion of boron atoms in graphite.

The difference in the experimental values of the diffusion constant perpendicular and parallel to the basal plane can be explained based on this model. Taking the barriers from the calculated kick-out path, the probability of a diffusion event parallel to the basal plane is a thousand times the probability of a diffusion event perpendicular to the basal plane at 2073 K. A parallel diffusion event requires the migration of the boron interstitial (0.8 eV), while the perpendicular event requires that the boron interstitial kicks back into the layer (2.3 eV).

The most plausible mechanism of boron diffusion in graphite is an interstitialcy or kick-out mechanism, which has the lowest energy barrier for the diffusion parallel and perpendicular to the basal pane. The prefactors are markedly different for the boron diffusion parallel and perpendicular to the basal plane because each kick-out event can allow only one diffusion step along the **c** direction (of $\mathbf{c}/2$) but many steps parallel to the basal plane due to the high mobility of the boron interstitial.

The activation energy is controlled by the formation and migration of carbon self-interstitials, and this explains the widely accepted similarity between diffusion rates for boron and carbon in graphite. Boron impurities in graphite trap point defects, such as vacancies and self-interstitial atoms.

Thanks are due particularly to A. J. Wickham and M. R. Bradford. We gratefully acknowledge support from British Energy Generation Ltd. The views expressed in this Letter are those of the authors and do not necessarily represent the views of British Energy Generation Ltd.

*Electronic address: is25@sussex.ac.uk

[1] C. E. Lowell, J. Am. Ceram. Soc. **50**, 142 (1967).
[2] G. R. Hennig, J. Chem. Phys. **42**, 1167 (1965).
[3] J. E. Brocklehurst, B. T. Kelly, and K. E. Gilchrist, Chem. Phys. Carbon **17**, 175 (1981).
[4] M. Endo, C. Kim, K. Nishimura, T. Fujino, and K. Miyashita, Carbon **38**, 183 (2000).
[5] K. Nishimura and M. Endo, U.S. Patent No. 6,946,110 (2005).
[6] P. A. Thrower and R. M. Mayer, Phys. Status Solidi (a) **47**, 11 (1978).
[7] L. M. Brown, A. Kelly, and R. M. Mayer, Philos. Mag. **19**, 721 (1969).
[8] W. N. Reynolds and P. A. Thrower, J. Nucl. Mater. **10**, 209 (1963).
[9] K. Niwase, Philos. Mag. Lett. **82**, 401 (2002).
[10] P. R. Goggin and W. N. Reynolds, Philos. Mag. **8**, 265 (1963).
[11] L. Bochirol, E. Bonjour, and L. Weil, *Radiation Damage in Reactor Materials* (International Atomic Energy Agency, Vienna, 1963).
[12] M. A. Kanter, Phys. Rev. **107**, 655 (1957).
[13] P. R. Briddon and R. Jones, Phys. Status Solidi (b) **217**, 131 (2000).
[14] H. J. Monkhorst and J. D. Pack, Phys. Rev. B **13**, 5188 (1976).
[15] M. Endo, T. Hayashi, S. Hong, T. Enoki, and M. S. Dresselhaus, J. Appl. Phys. **90**, 5670 (2001).
[16] A. A. El-Barbary, R. H. Telling, C. P. Ewels, M. I. Heggie, and P. R. Briddon, Phys. Rev. B **68**, 144107 (2003).
[17] A. V. Krasheninnikov and V. F. Elesin, Surf. Sci. **454–456**, 519 (2000).
[18] R. H. Telling and M. I. Heggie, Philos. Mag. **83**, 411 (2003).
[19] V. Serin, R. Brydson, A. Scott, Y. Kihn, O. Abidate, B. Maquin, and A. Derre, Carbon **38**, 547 (2000).
[20] J. R. Manning, *Diffusion Kinetics for Atoms in Crystals* (D. Van Nostrand Company, Inc., London, 1968).
[21] E. Kaxiras and K. C. Pandey, Phys. Rev. Lett. **61**, 2693 (1988).
[22] C. H. Xu, C. L. Fu, and D. F. Pedraza, Phys. Rev. B **48**, 13 273 (1993).